

# Measurement report: Oxidation potential of water-soluble aerosol components in the southern and northern of Beijing

Wei Yuan<sup>1</sup>, Ru-Jin Huang<sup>1</sup>, Chao Luo<sup>2</sup>, Lu Yang<sup>1</sup>, Wenjuan Cao<sup>1</sup>, Jie Guo<sup>1</sup>, Huinan Yang<sup>2</sup>

<sup>1</sup>State Key Laboratory of Loess and Quaternary Geology, Center for Excellence in Quaternary Science and Global Change, Institute of Earth Environment, Chinese Academy of Sciences, Xi'an 710061, China.

<sup>2</sup>School of Energy and Power Engineering, University of Shanghai for Science and Technology, Shanghai 200093, China

Correspondence: Ru-Jin Huang (rujin.huang@ieecas.cn) and Huinan Yang (yanghuinan@usst.edu.cn)

## Abstract

Water-soluble components have significant contribution to the oxidative potential (OP) of atmospheric fine particles (PM<sub>2.5</sub>), while our understanding of water-soluble PM<sub>2.5</sub> OP and its sources, as well as its relationship with water-soluble components, is still limited. In this study, the water-soluble OP levels in wintertime PM<sub>2.5</sub> in the south and north of Beijing, representing the difference in sources, were measured with dithiothreitol (DTT) assay. The volume normalized DTT (DTT<sub>v</sub>) in the north ( $3.5 \pm 1.2 \text{ nmol min}^{-1} \text{ m}^{-3}$ ) was comparable to that in the south ( $3.9 \pm 0.9 \text{ nmol min}^{-1} \text{ m}^{-3}$ ), while the mass normalized DTT (DTT<sub>m</sub>) in the north ( $65.3 \pm 2827.6 \text{ pmol min}^{-1} \mu\text{g}^{-3}$ ) was almost twice that in the south ( $36.1 \pm 14.5 \text{ pmol min}^{-1} \mu\text{g}^{-3}$ ). In both the south and north of Beijing, DTT<sub>v</sub> was better correlated with soluble elements instead of total elements. In the north, soluble elements (mainly Mn, Co, Ni, Zn, As, Cd and Pb) and water-soluble organic compounds, especially light-absorbing compounds (also known as brown carbon), had positive correlations with DTT<sub>v</sub>.

29 However, in the south, the DTT<sub>v</sub> was mainly related to soluble As, Fe and Pb. The  
30 sources of DTT<sub>v</sub> were further resolved using the positive matrix factorization (PMF)  
31 model. Traffic-related emissions (39.1%) and biomass burning (25.2%) were the main  
32 sources of DTT<sub>v</sub> in the south, and traffic-related emissions (> 50%) contributed the  
33 most of DTT<sub>v</sub> in the north. Our results indicate that vehicle emission was the  
34 important contributor to OP in Beijing ambient PM<sub>2.5</sub> and suggest that more study is  
35 needed to understand the intrinsic relationship between OP and light absorbing  
36 organic compounds.

37

## 38 **1 Introduction**

39 Atmospheric fine particulate matter (PM<sub>2.5</sub>) pollution is one of the major global  
40 environmental issues, affecting air quality, climate and human health (Huang et al.,  
41 2014; Burnett et al., 2018; An et al., 2019; Zheng et al., 2020). The exposure to PM<sub>2.5</sub>  
42 was estimated to be responsible for 8.9 million deaths worldwide in 2015, of which  
43 28% occurred in China (Burnett et al., 2018). Numerous studies have shown that  
44 oxidative stress is one of the main mechanisms underlying the adverse effects of  
45 PM<sub>2.5</sub> on human health (Chowdhury et al., 2019; Lelieveld et al., 2021; Yu et al.,  
46 2022b). When entering the human body, PM<sub>2.5</sub> can induce the production of excessive  
47 reactive oxygen species (ROS) (e.g., H<sub>2</sub>O<sub>2</sub>, ·OH and ·O<sub>2</sub><sup>-</sup>), leading to cellular redox  
48 imbalance and generating oxidative stress effects. The ability of PM<sub>2.5</sub> to cause  
49 oxidative stress is defined as oxidative potential (OP).

50 The methods to determine the OP of PM<sub>2.5</sub> include cellular and acellular assays,  
51 and acellular methods are more widely used than cellular methods (Charrier and  
52 Anastasio, 2012; Xiong et al., 2017; Calas et al., 2018; Bates et al., 2019; Wang et al.,  
53 2020b; Campbell et al., 2021; Oh et al., 2023). Among acellular methods, the  
54 dithiothreitol (DTT) assay is extensively applied to determine the OP of ambient  
55 particles (Charrier and Anastasio, 2012; Xiong et al., 2017; Liu et al., 2018; Wang et  
56 al., 2020b; Puthussery et al., 2022; Wu et al., 2022a). DTT is a surrogate of cellular  
57 reductants, and the consumption rate of DTT was used to assess the OP of PM<sub>2.5</sub>.

58 Previous studies have shown that organic matters (e.g., water-soluble organic species  
59 and PAHs) and some transition metals (e.g., Mn and Cu) are the important  
60 contributors to DTT consumption of PM<sub>2.5</sub> (Charrier and Anastasio, 2012; Verma et  
61 al., 2015; Bates et al., 2019; Wu et al., 2022a; Wu et al., 2022b). For example,  
62 Charrier and Anastasio (2012) measured the OP of PM<sub>2.5</sub> in San Joaquin Valley,  
63 California and reported that about 80% of DTT consumption was contributed by  
64 transition metals. Verma et al. (2015) measured the OP of water-soluble PM<sub>2.5</sub> in the  
65 southeastern United States and reported that about 60% of DTT activity was  
66 contributed by water-soluble organics. The mixtures of metals and organics may  
67 produce synergistic or antagonistic effects, such as ·O<sub>2</sub><sup>-</sup> produced from oxidation of  
68 DTT by quinones is more efficiently transformed to ·OH in the presence of Fe, while  
69 the DTT consumption and ·OH generation of quinones are reduced in the presence of  
70 Cu (Xiong et al., 2017; Yu et al., 2018; Bates et al., 2019).

71 A number of studies have investigated the OP of water-soluble components in  
72 PM<sub>2.5</sub>, which show that the average water-soluble OP values in urban areas ranged  
73 from 0.1 to 10 nmol min<sup>-1</sup> m<sup>-3</sup> (Fang et al., 2016; Liu et al., 2018; Chen et al., 2019;  
74 Wu et al., 2022a; Yu et al., 2022a; Xing et al., 2023). Due to the complexity in  
75 chemical composition and sources of PM<sub>2.5</sub> that determine the OP levels, the sources  
76 of OP are also diverse (Verma et al., 2015; Bates et al., 2019; Tuet et al., 2019; Yu et  
77 al., 2019; Cao et al., 2021). Several studies have investigated the emission sources and  
78 ambient samples to identify the sources of OP (Tuet et al., 2019; Yu et al., 2019; Wang  
79 et al., 2020b; Cao et al., 2021), which include both primary and secondary sources.  
80 For example, Cao et al. (2021) measured the water-soluble OP of PM<sub>2.5</sub> samples from  
81 six biomass and five coal burning emissions in China, with average values of 4.5-7.4  
82 and 0.5-2.1 pmol min<sup>-1</sup> μg<sup>-1</sup>, respectively. Tong et al. (2018) investigated the OP of  
83 secondary organic aerosols (SOA) from oxidation of naphthalene, isoprene and β-  
84 pinene with ·OH or O<sub>3</sub>, which were 104.4 ± 7.6, 48.3 ± 7.9 and 36.4 ± 3.1 pmol min<sup>-1</sup>  
85 μg<sup>-1</sup>, respectively. Verma et al. (2014) identified the sources of water-soluble OP of  
86 PM<sub>2.5</sub> in Atlanta, United States from June 2012 to September 2013 with positive

87 matrix factorization (PMF) and chemical mass balance (CMB) methods, of which  
88 biomass burning was the largest contributor. Wang et al. (2020b) quantified the  
89 sources of water-soluble OP of PM<sub>2.5</sub> in Xi'an, China in 2017 using PMF and multiple  
90 linear regression (MLR) methods, with significant contributions from secondary  
91 sulfates, vehicle emissions and coal combustion. Despite these efforts, comparative  
92 studies on the differences in pollution levels and sources of PM<sub>2.5</sub> OP in different  
93 districts are still limited.

94 In this study, the DTT activity of water-soluble matter in PM<sub>2.5</sub> samples collected  
95 simultaneously in the southern and northern of Beijing in January 2018 were  
96 measured. The concentration and light absorption of water-soluble organic carbon  
97 (WSOC), as well as the concentrations of 14 trace elements and 7 light-absorbing  
98 nitroaromatic compounds (NACs) were quantified. The sources of DTT activity were  
99 then identified with PMF model. The results acquired in this study provide a  
100 comparison of PM<sub>2.5</sub> OP in different districts of Beijing and its connection with  
101 organic compounds, trace elements and sources, which could be helpful for further  
102 study of the regional differences in the effects of PM<sub>2.5</sub> on human health.

103

## 104 **2 Materials and methods**

### 105 **2.1 Sampling**

106 Ambient 24 h integrated PM<sub>2.5</sub> filter samples were collected from January 1 to 31,  
107 2018 simultaneously in the south (the Dingfuzhuang village (DFZ), Daxing district;  
108 39.61°N, 116.28°E) and north (the National Center for Nanoscience and Technology  
109 (NCNT), Haidian district; 39.99°N, 116.32°E) of Beijing (Figure S1). The distance  
110 between the two sampling sites is about 42 km. The south site is surrounded by  
111 agricultural, industrial, and transportation areas, and the north site is surrounded by  
112 residential, transportation and commercial areas. PM<sub>2.5</sub> samples were collected on pre-  
113 baked (780 °C, 3 h) quartz-fiber filters (20.3 × 25.4 cm; Whatman, QM-A, Clifton, NJ,  
114 USA) using high-volume PM<sub>2.5</sub> samplers (1.13 m<sup>3</sup> min<sup>-1</sup>; Tisch, Cleveland, OH, USA)  
115 which were placed on the roof of buildings at heights of about 5 m (south) and 20 m

116 (north) above the ground. 31 samples were collected at each site. After collection, the  
117 samples were wrapped in baked aluminum foils and stored in a freezer ( $-20\text{ }^{\circ}\text{C}$ ) until  
118 further analysis.

## 119 **2.2 Chemical analysis**

120 The mass of  $\text{PM}_{2.5}$  on the filter was measured by a digital microbalance with a  
121 precision of 0.1 mg (LA130S-F, Sartorius, Germany) after 24-h equilibration at a  
122 constant temperature ( $20\text{-}23\text{ }^{\circ}\text{C}$ ) and humidity (35-45%) chamber. Each filter was  
123 weighted at least two times, and the deviations for blank and sampled filters among  
124 the repetitions were less than 5 and 10  $\mu\text{g}$ , respectively. The  $\text{PM}_{2.5}$  mass concentration  
125 was calculated by dividing the weight difference before and after sampling by the  
126 volume of sampled air.

127 For WSOC analysis, one punch ( $1.5\text{ cm}^2$  for concentration analysis and  $0.526$   
128  $\text{cm}^2$  for light absorption measurement) of filter was taken from each sample and  
129 extracted ultrasonically with ultrapure water ( $> 18.2\text{ M}\Omega\text{ cm}$ ) for 30 min. After, the  
130 extracts were filtered with a  $0.45\text{ }\mu\text{m}$  PVDF pore syring filter to remove insoluble  
131 substances. Finally, the concentration of WSOC was measured with a total organic  
132 carbon-total nitrogen analyzer (TOC-L, Shimadzu, Japan; (Ho et al., 2015)) and the  
133 light absorption of WSOC was measured by an UV-Vis spectrophotometer ( $300\text{-}700$   
134 nm; Ocean Optics, USA) equipped with a liquid waveguide capillary cell (LWCC-  
135 3100, World Precision Instruments, Sarasota, FL, USA; (Yuan et al., 2020)). The  
136 absorption coefficient (Abs) of WSOC was calculated according to formula S1 in the  
137 Supporting Information (SI).

138 The total concentration and soluble fraction concentration of 14 trace elements  
139 (i.e., Ti, V, Cr, Mn, Fe, Co, Ni, Cu, Zn, As, Sr, Cd, Ba, and Pb) were quantified by an  
140 inductively coupled plasma mass spectrometer (ICP-MS, 7700x, Agilent Technologies,  
141 USA), and the details are shown in the SI. For soluble fraction concentration analysis,  
142 a punch of filter ( $47\text{ mm}$  diameter) was extracted with ultrapure water and then  
143 centrifuged from residues. For total concentration analysis, another  $47\text{ mm}$  diameter  
144 filter of the same sample was used and digested with  $10\text{ mL HNO}_3$  and  $1\text{ mL HF}$  at

145 180 °C for 12 h. The extracts were then heated and concentrated to ~ 0.1 mL, and  
146 diluted to 5 mL with 2% HNO<sub>3</sub>. Afterwards, the diluents were filtered with a 0.22 µm  
147 PTFE pore syring filter and stored in a freezer (-4 °C) until further ICP-MS analysis.

148 The concentrations of organic markers (including levoglucosan, mannosan,  
149 galactosan, hopanes (including 17α(H)-22,29,30-trisnorhopane, 17α(H),21β(H)-30-  
150 norhopane, 17β(H),21α(H)-30-norhopane, 17β(H),21α(H)-hopane, 17β(H),21α(H)-  
151 hopane and 17β(H),21α(H)-hopane), picene, phthalic acid, isophthalic acid and  
152 terephthalic acid) and light-absorbing NACs (including 4-nitrophenol (4NP), 2-  
153 methyl-4-nitrophenol (2M4NP), 3-methyl-4-nitrophenol (3M4NP), 4-nitrocatechol  
154 (4NC), 3-methyl-5-nitrocatechol (3M5NC), 4-methyl-5-nitrocatechol (4M5NC) and  
155 4-nitro-1-naphthol (4N1N)) were determined by a gas chromatograph–mass  
156 spectrometer (GC-MS; Agilent Technologies, Santa Clara, CA, USA) following the  
157 method described elsewhere (Wang et al., 2020a), and more details about the analysis  
158 can be found in SI. All of the results reported in this study were corrected for blanks.

### 159 **2.3 Oxidative potential**

160 The DTT assay was applied to determine the oxidative potential of water-soluble  
161 components in PM<sub>2.5</sub> according to the method by Gao et al. (2017). In brief, a quarter  
162 of a 47 mm filter was ultrasonically extracted with 5 mL ultrapure water for 30 min  
163 and then filtered with a 0.45 µm PVDF pore syring filter to remove insoluble  
164 substances. Several studies have shown that ultrasonic treatment of samples can lead  
165 to an increase in ~~their~~ OP values (Miljevic et al., 2014; Jiang et al., 2019), however,  
166 there was also a study showed that the difference in OP values of water-soluble PM<sub>2.5</sub>  
167 measured by DTT assay was little for samples extracted by ultrasonic and shaking  
168 (Gao et al., 2017). Consistent with the extraction methods ~~of~~ for organic markers and  
169 trace elements ~~analysis~~, ultrasonic method was used to extract samples for DTT  
170 analysis. Afterwards, 0.5 mL of the extract was mixed with 1 mL of potassium  
171 phosphate buffer (pH = 7.4) and 0.5 mL of 2 mM DTT in a brown vial, and then  
172 placed in a water bath at 37 °C. Then, 20 µL of this mixture was taken at designated  
173 time intervals (2, 7, 13, 20, and 28 min) and mixed with 1 mL trichloroacetic acid

174 (TCA; 1% w/v) in another brown vial to terminate the reaction. Then, 0.5 mL of 5,5'-  
175 dithiobis-(2-nitrobenzoic acid) (DTNB; 2.5  $\mu\text{M}$ ) and 2 mL of tris buffer (pH = 8.9)  
176 were added to form 2-nitro-5-thiobenzonic acid (TNB) which has light absorption at  
177 412 nm. Finally, the absorption of TNB was measured by a LWCC-UV-Vis. The DTT  
178 consumption rate was quantified by the remaining DTT concentration at different  
179 reaction times. Daily solution blanks and filter blanks were analyzed in parallel with  
180 samples to evaluate the consistency of the system performance. Besides, for every 10  
181 samples, one sample was chosen to be measured three times to check the  
182 reproducibility, and the relative standard deviation was lower than 5%. Ambient  
183 samples were corrected for filter blank. The DTT activities were normalized by the  
184 volume of sampled air ( $\text{DTT}_v$ ,  $\text{nmol min}^{-1} \text{m}^{-3}$ ) and the mass concentration of  $\text{PM}_{2.5}$   
185 ( $\text{DTT}_m$ ,  $\text{pmol min}^{-1} \mu\text{g}^{-1}$ ).

186 Considering that for samples containing a with significant amount of substances  
187 contributions from species whose DTT response is non-linear with related to  $\text{PM}_{2.5}$   
188 concentration (e.g., Cu, Mn), the  $\text{DTT}_m$  value depends on the concentration of  
189  $\text{PM}_{2.5}$  in added to the reaction solution extraction solution (Charrier et al., 2016). The  
190 response of  $\text{DTT}_m$  to  $\text{PM}_{2.5}$  concentration added to in the extraction-reaction solution  
191 was analyzed using sample containing with high concentrations of soluble Cu and Mn  
192 (Figure S2). In the range of When the  $\text{PM}_{2.5}$  concentrations added to the reaction  
193 solution is less than  $150 \mu\text{g mL}^{-1}$ , the  $\text{DTT}_m$  response was is greatly affected by the  
194 difference in added  $\text{PM}_{2.5}$  concentrations; however, when the concentrations of  $\text{PM}_{2.5}$   
195 concentration added to in the reaction solution is extract were greater than  $150 \mu\text{g mL}^{-1}$ ,  
196 the  $\text{DTT}_m$  response is less affected by the difference in  $\text{PM}_{2.5}$  concentration changed  
197 little ( $< 12\%$ ) with the increase of  $\text{PM}_{2.5}$  concentrations. In this study, the  
198 concentrations of  $\text{PM}_{2.5}$  added to in the reaction extraction solution of most samples  
199 from the two sites were was greater than  $150 \mu\text{g mL}^{-1}$  (ranged from 7978.7 to  
200 749748.7  $\mu\text{g mL}^{-1}$ , with an average values of 409408.9  $\pm 164.1$  and 207206.6  $\pm 95.0$   
201  $\mu\text{g mL}^{-1}$  in the south and north, respectively), therefore, the difference in  $\text{PM}_{2.5}$   
202 concentrations added to the reaction solution of in different samples extracts should

203 had a relatively small impact on the difference in DTT<sub>m</sub> values of ~~different the~~  
204 samples. This study did not consider the impact of metal precipitation in phosphate  
205 matrix on the measured DTT values, as there is ~~not~~ a straightforward method to  
206 correct the artifacts caused by this phenomenon (Yalamanchili et al., 2023).

## 207 **2.4 Source apportionment**

208 The sources of DTT activities were identified and quantified using PMF model  
209 implemented by the multilinear engine (ME-2; (Paatero, 1997)) following the method  
210 described in our previous studies (Huang et al., 2014; Yuan et al., 2020). ~~For each site,~~  
211 ~~31 samples and 23 species were input into PMF model. A total of 62 samples and 23~~  
212 ~~species were input into PMF model.~~ The number of samples is higher than the number  
213 of species, ~~and approaching the ratio of at least 3:1 proposed by Belis et al. (2019).~~  
214 The input data include species concentration (including DTT<sub>v</sub>, 14 trace elements and  
215 8 organic markers) and uncertainties. The species-specific uncertainties were  
216 calculated following Liu et al. (2017). More details are described in SI (PMF analysis).

## 217 218 **3 Results and discussion**

### 219 **3.1 DTT activity and concentrations of water-soluble PM<sub>2.5</sub> components**

220 Figure 1 shows the daily variation of DTT activity, light absorption of WSOC at  
221 wavelength 365 nm (Abs<sub>365</sub>), together with the concentrations of PM<sub>2.5</sub>, WSOC,  
222 NACs and total elements in the south and north of Beijing. Their average values are  
223 shown in Table S1. Generally, the average values of PM<sub>2.5</sub>, WSOC, Abs<sub>365</sub>, NACs and  
224 total elements were higher in the south than in the north. Specifically, the  
225 concentrations of PM<sub>2.5</sub> and WSOC in the south (~~122.3 ± 4948.9~~  $122.3 \pm 4948.9$   $\mu\text{g m}^{-3}$  and  $8.1 \pm 5.0$   
226  $\mu\text{gC m}^{-3}$ , respectively) were both about two times higher than that in the north (~~62.3 ±~~  
227 ~~2827.9~~  $62.3 \pm 2827.9$   $\mu\text{g m}^{-3}$  and  $4.0 \pm 2.0$   $\mu\text{gC m}^{-3}$ , respectively), indicating that the proportion of  
228 WSOC in PM<sub>2.5</sub> was similar in the south and north. However, the Abs<sub>365</sub> in the south  
229 was about three times that in the north, indicating that the chemical composition of  
230 WSOC was different between the south and north. Previous studies have reported that  
231 NACs are the main water-soluble light-absorbing organic compounds (also known as



232 brown carbon, BrC) of PM<sub>2.5</sub> (Lin et al., 2017; Huang et al., 2020; Li et al., 2020). For  
233 the 7 NACs quantified in this study, the total concentration of nitrophenols (4NP,  
234 2M4NP and 3M4NP), nitrocatechols (4NC, 3M5NC and 4M5NC), and 4N1N in the  
235 south ( $108.5 \pm 7372.9$  ng m<sup>-3</sup>,  $118.5 \pm 91.5$  ng m<sup>-3</sup> and  $12.4 \pm 8.2$  ng m<sup>-3</sup>, respectively)  
236 was about three, five and four times, respectively, those in the north ( $35.5 \pm 2221.7$  ng  
237 m<sup>-3</sup>,  $24.1 \pm 30.4$  ng m<sup>-3</sup> and  $3.1 \pm 3.0$  ng m<sup>-3</sup>, respectively). These results indicate that  
238 the sources and emission strength of water-soluble organic compounds were different  
239 in the south and north of Beijing, suggesting the different contribution of water-  
240 soluble organic compounds to DTT activity. The concentration trends of trace  
241 elements were also different between the south and north of Beijing, with Fe >  
242 Zn > Ti > Mn > Cu > Ba > Pb > Sr > Cr > As > V > Ni > Cd > Co in the south, and  
243 Fe > Ti > Zn > Ba > Mn > Pb > Cu > Cr > Sr > As > Ni > V > Cd > Co in the north. It  
244 should be noted that although the contents of PM<sub>2.5</sub>, WSOC and total elements  
245 measured in this study were higher in the south than in the north, the average DTT<sub>v</sub>  
246 value in the south ( $3.9 \pm 0.9$  nmol min<sup>-1</sup> m<sup>-3</sup>) was comparable to that in the north ( $3.5$   
247  $\pm 1.2$  nmol min<sup>-1</sup> m<sup>-3</sup>), meanwhile, the average DTT<sub>m</sub> value was much higher (1.8  
248 times) in the north ( $65.3 \pm 2827.6$  pmol min<sup>-1</sup> μg<sup>-1</sup>) than in the south ( $36.1 \pm 14.5$   
249 pmol min<sup>-1</sup> μg<sup>-1</sup>). The lower DTT<sub>m</sub> in the south than in the north may be due to the  
250 increased PM<sub>2.5</sub> in the south containing more substances with no or little contribution  
251 to DTT activity, and indicates that the intrinsic OP of water-soluble components of  
252 PM<sub>2.5</sub> was higher in the north than in the south. The similar DTT<sub>v</sub> values in the south  
253 and north indicate that the exposure-relevant OP of water-soluble components of  
254 PM<sub>2.5</sub> was comparable in the two sites, and the water-soluble DTT<sub>v</sub> was not consistent  
255 with the content of water-soluble substances.

256 Figure 2 shows the comparison of water-soluble PM<sub>2.5</sub> DTT activity measured in  
257 this study with those measured in other regions of Asia during similar periods. It can  
258 be seen that the DTT<sub>v</sub> values measured in Beijing in this study were lower than that in  
259 Jinzhou, Tianjin, Yantai, and Shanghai in China, Lahore and Peshawar in Pakistan,  
260 and Delhi in India (Liu et al., 2018; Ahmad et al., 2021; Puthussery et al., 2022; Wu et

261 al., 2022a), higher than that in Xi'an, Nanjing, Hangzhou, Guangzhou, and Shenzhen  
262 in China (Wang et al., 2019; Wang et al., 2020b; Ma et al., 2021; Yu et al., 2022c;  
263 Xing et al., 2023), and comparable with that in Ningbo, China (Chen et al., 2022).  
264 Different from  $DTT_v$ , the  $DTT_m$  value measured in NCNT in Beijing was similar with  
265 that in Jinzhou, Tianjin, Yantai, Shanghai and Ningbo in China (Liu et al., 2018; Chen  
266 et al., 2022; Wu et al., 2022a), and higher than that in other regions. The differences in  
267 water-soluble DTT activity of  $PM_{2.5}$  in different regions can be explained by the  
268 differences in chemical composition, sources and atmospheric formation processes  
269 (Tong et al., 2017; Wong et al., 2019; Daellenbach et al., 2020; Wang et al., 2020b;  
270 Cao et al., 2021). For example, Cao et al. (2021) reported the water-soluble DTT  
271 activity of  $PM_{2.5}$  from biomass and coal burning emissions in China, and the average  
272 value of biomass burning ( $4.5-7.4 \text{ pmol min}^{-1} \mu\text{g}^{-1}$ ) was much higher than that of coal  
273 burning ( $0.5-2.1 \text{ pmol min}^{-1} \mu\text{g}^{-1}$ ). Tuet et al. (2017) measured the water-soluble DTT  
274 activity of SOA generated under different precursors and reaction conditions, with  
275 SOA from naphthalene photooxidation under  $RO_2 + NO$ -dominant dry reaction  
276 conditions had the highest DTT activity.

### 277 **3.2 Correlation between DTT activity and water-soluble $PM_{2.5}$ components**

278 Figure 3 shows the correlations of  $DTT_v$  with  $PM_{2.5}$ , WSOC and  $Ab_{S_{365}}$  in the  
279 south and north of Beijing. It can be seen that the correlation coefficient between  
280  $DTT_v$  and  $PM_{2.5}$  was moderate in both the south ( $r = 0.42$ ) and north ( $r = 0.45$ ),  
281 indicating that the toxicity of particles cannot be evaluated solely by the total  $PM_{2.5}$   
282 concentration. The correlations between  $DTT_v$  with WSOC and  $Ab_{S_{365}}$  were strong in  
283 the north ( $r$  of 0.69 and 0.70, respectively), while relatively weak in the south ( $r$  of  
284 0.41 and 0.40, respectively). The high correlations between  $DTT_v$  with WSOC and  
285  $Ab_{S_{365}}$  in the north of Beijing qualitatively agree with previous studies in Xi'an, China  
286 and Atlanta, United States (Verma et al., 2012; Chen et al., 2019), and suggest that  
287 water-soluble organic matter, especially BrC, has a significant contribution to DTT  
288 consumption in the north. Light-absorbing BrC typically has conjugated electrons,  
289 making it more likely to transport electrons for catalytic reactions, thereby

290 contributing to DTT activity (Chen et al., 2019; Wu et al., 2022). Further, in the north,  
291 the  $DTT_v$  was closely related to the concentrations of NACs ( $r$  of 0.57 to 0.79) (Figure  
292 S3), suggesting that NACs may be important contributors to DTT consumption. Feng  
293 et al. (2022) reported the positive correlations between NACs and biomarkers in  
294 saliva and urine (interleukin-6 and 8-hydrox-2'-deoxyguanosine). Zhang et al. (2023)  
295 also reported that NACs are major proinflammatory components in organic aerosols,  
296 contributing about 24% of the interleukin-8 response of all compounds detected by  
297 Fourier transform ion cyclotron resonance mass spectrometry (FT-ICR-MS) in  
298 electrospray ionization negative mode (ESI-). Certainly, it may also be other  
299 substances related to NACs that contribute to the DTT activity, including those not  
300 detected in this study, driving the good correlation between NACs and  $DTT_v$  in the  
301 north of Beijing, which is worth studying in the future.

302 The correlation coefficients between  $DTT_v$  and 14 trace elements are shown in  
303 Figure 4. Generally, the correlations between  $DTT_v$  and soluble elements were higher  
304 than that between  $DTT_v$  and total elements in both the south and north of Beijing. For  
305 soluble elements, in the south, the  $DTT_v$  showed positive correlations with Mn, Fe, Cr,  
306 Co, As and Pb ( $r > 0.5$ ), while in the north, it exhibited strong positive correlations  
307 with Mn, Co, Ni, Zn, As, Cd and Pb ( $r > 0.7$ ), indicating the different sources of  $DTT_v$   
308 in the south and north of Beijing. It is worth noting that the concentrations of all  
309 soluble elements were higher in the south than in the north (Figure S4), while the  
310 correlation between  $DTT_v$  and most soluble elements was lower in the south than in  
311 the north (Figure 4). The high correlations between  $DTT_v$  and soluble elements in the  
312 north of Beijing suggests that soluble elements also had a significant contribution to  
313 DTT consumption. The low correlations between  $DTT_v$  and soluble elements in the  
314 south of Beijing may be due to the nonlinear relationship between DTT consumption  
315 and elements concentrations (Charrier and Anastasio, 2012; Wu et al., 2022a). As  
316 shown in Figure S5, the relationship between most soluble trace elements and  $DTT_v$   
317 was more non-linear than linear. As the concentration of soluble elements increases,  
318 the growth rate of  $DTT_v$  obviously decreases.

319 In addition to being associated with individual water-soluble species, the  
320 interactions between metals and organic compounds also affect the consumption of  
321 DTT (Xiong et al., 2017; Wu et al., 2022b), with both synergistic and antagonistic  
322 effects. For example, Wu et al. (2022b) measured the DTT consumption of Fe(III) and  
323 Cu(II) interacting with 1,4-naphthoquinone, 9,10-phenanthraquinone, citric acid, and  
324 4-nitrocatechol, respectively. Their results showed that Cu(II) had antagonistic effects  
325 in interacting with most organics except for citric acid, and Fe(III) had an additive  
326 effect on DTT consumption of 1,4-naphthoquinone and citric acid, while it had an  
327 antagonistic effect on 1,4-naphthoquinone and 9,10-phenanthraquinone. Due to the  
328 complex composition of water-soluble organic aerosols, the knowledge about the  
329 effects of organics and metal-organic interactions on DTT activity are still limited,  
330 especially the effects of BrC chromophores and their interactions with metals.

### 331 **3.3 Sources of DTT activity**

332 This study analyzed eight organic markers (including levoglucosan, mannosan,  
333 and galactosan for biomass burning, hopanes for vehicle emissions, picene for coal  
334 combustion, and phthalic acid, isophthalic acid and terephthalic acid for secondary  
335 formation) to help identify the sources of DTT activity. The correlation coefficients  
336 between  $DTT_v$  and organic markers are shown in Figure S65. In the south,  
337 levoglucosan, mannosan, galactosan, and hopanes had moderate correlation with  
338  $DTT_v$  (r of 0.41 to 0.48); phthalic acid, isophthalic acid and terephthalic acid had low  
339 to moderate correlation with  $DTT_v$  (r of 0.28 to 0.54); picene had low correlation with  
340  $DTT_v$  (r of 0.21). These results suggest that biomass burning and vehicle emissions  
341 could have significant contribution to water-soluble  $PM_{2.5}$  OP in the south. In the  
342 north, hopanes had the highest correlation with  $DTT_v$  ( $r = 0.70$ ), indicating that  
343 vehicle emissions could have an important contribution. Levoglucosan, mannosan,  
344 galactosan, phthalic acid, isophthalic acid, terephthalic acid, and picene had moderate  
345 to high correlations with  $DTT_v$  in the north, suggesting that biomass and coal burning,  
346 and secondary formation may also have certain contribution to water-soluble  $PM_{2.5}$   
347 OP.

348 To further quantify the sources of DTT activity in the south and the north of  
349 Beijing, the PMF model, which was widely used for the source apportionment of  
350 PM<sub>2.5</sub> OP (Liu et al., 2018; Shen et al., 2022; Cui et al., 2023), was applied. The input  
351 species include DTT<sub>v</sub>, soluble elements and organic markers, and five to seven factors  
352 were examined. Due to the oil factor mixed with vehicle emissions factor in the five-  
353 factor solution, and there was no new reasonable factor when increasing the factor  
354 number to seven in the PMF analysis (Figure S76). Finally, six factors were resolved  
355 and quantified using PMF model in the south and north of Beijing, including biomass  
356 burning, coal burning, traffic-related, dust, oil combustion, and secondary formation,  
357 and the profiles of these sources are shown in Figure S87. Factor 1 is characterized by  
358 high contribution of levoglucosan, mannosan, and galactosan, mainly from biomass  
359 burning (Huang et al., 2014; Chow et al., 2022). The DTT activity of biomass burning  
360 organic aerosol was measured by Wong et al. (2019), which was  $48 \pm 6 \text{ pmol min}^{-1}$   
361  $\mu\text{g}^{-1}$  of WSOC. Liu et al. (2018) quantified the sources of DTT<sub>v</sub> in coastal cities  
362 (Jinzhou, Tianjin, and Yantai) in China with PMF model and multiple linear  
363 regression method, and the results showed that biomass burning contributed 27.828%  
364 on average in winter. Factor 2 exhibits a large fraction of picene, Zn, Mn, Cd, As, and  
365 Pb, which is considered to be coal burning (Huang et al., 2014; Huang et al., 2018).  
366 Joo et al. (2018) measured the DTT activity of PM<sub>2.5</sub> emitted from coal combustion at  
367 different temperatures, with the highest values of  $26.2 \pm 2120.5 \text{ pmol min}^{-1} \mu\text{g}^{-1}$  and  
368  $0.10 \pm 0.06 \text{ nmol min}^{-1} \text{ m}^{-3}$  occurring at 550 °C. Factor 3 is identified as traffic-related  
369 emissions, which is characterized by the higher loading of hopanes, Ba, Sr, Cu and Ni  
370 (Huang et al., 2018; Chow et al., 2022). Vreeland et al. (2017) measured the DTT  
371 activity of PM<sub>2.5</sub> emitted by side street and highway vehicles in Atlanta, with values  
372 of  $0.78 \pm 0.60 \text{ nmol min}^{-1} \text{ m}^{-3}$  and  $1.14.08 \pm 0.60 \text{ nmol min}^{-1} \text{ m}^{-3}$ , respectively. Ting et  
373 al. (2023) reported that the DTT activity of PM<sub>2.5</sub> from vehicle emissions in Ziqing  
374 tunnel in Taiwan, China, was 0.15-0.46 nmol min<sup>-1</sup> m<sup>-3</sup>. Factor 4, secondary formation,  
375 which is identified by high levels of phthalic acid, isophthalic acid, and terephthalic  
376 acid (Al-Naiema and Stone, 2017; Wang et al., 2020a). Verma et al. (2014) reported

377 that secondary formation contributed about 30% to the water-soluble DTT activity of  
378 PM<sub>2.5</sub> in urban Atlanta. It is worth noting that the DTT activity of SOA generated  
379 from different precursors is different (Tuet et al., 2017; Tong et al., 2018). For  
380 example, the DTT activity of SOA from naphthalene was higher than that from  
381 isoprene (Tuet et al., 2017; Tong et al., 2018). Factor 5 is dominated by crustal  
382 elements Fe and Ti, mainly from dust (Huang et al., 2018). The DTT activity of  
383 atmospheric particulate matter during dust periods were reported in previous studies  
384 (Chirizzi et al., 2017; Khoshnamvand et al., 2023) and it has a low contribution in this  
385 study. Factor 6 is identified as oil combustion because of the high levels of V and Ni  
386 (Moreno et al., 2011; Minguillón et al., 2014; Huang et al., 2018).

387 The source contributions of DTT<sub>v</sub> in the south and north of Beijing are shown in  
388 Figure 5, exhibiting obvious district differences. In the south, traffic-related emissions  
389 (39.4%) and biomass burning (25.2%) had the most contribution to DTT<sub>v</sub>, followed  
390 by secondary formation (17.2%), coal burning (15%), dust (2%), and oil combustion  
391 (4.52%). In the north, traffic-related emissions (51.652%) had the highest contribution  
392 to DTT<sub>v</sub>, followed by coal burning (19.920%), secondary formation (13%), biomass  
393 burning (8.4%), oil combustion (4.1%), and dust (3%). The absolute contribution of  
394 each source to DTT<sub>v</sub> varies by 1.2-3.4 times between the south and north of Beijing  
395 (Table S2). The large district differences in sources of DTT<sub>v</sub> of water-soluble PM<sub>2.5</sub>  
396 call for more research on the relationship between sources, chemical composition,  
397 formation processes and OP of PM<sub>2.5</sub>.

398

#### 399 4 Conclusions

400 In this study, the water-soluble OP of ambient PM<sub>2.5</sub> collected in winter in the  
401 south and north of Beijing were quantified, together with the concentration and light  
402 absorption of WSOC, and concentrations of 7 light-absorbing NACs and 14 trace  
403 elements. The average DTT<sub>v</sub> value was comparable in the south ( $3.9 \pm 0.9 \text{ nmol min}^{-1}$   
404  $\text{m}^{-3}$ ) and north ( $3.5 \pm 1.2 \text{ nmol min}^{-1} \text{ m}^{-3}$ ), while the DTT<sub>m</sub> was higher in the north  
405 ( $65.3 \pm 2827.6 \text{ pmol min}^{-1} \mu\text{g}^{-1}$ ) than in the south ( $36.1 \pm 14.5 \text{ pmol min}^{-1} \mu\text{g}^{-1}$ ),

406 indicating that the exposure-relevant OP of water-soluble components of PM<sub>2.5</sub> was  
407 similar in the two sites and that the intrinsic OP of water-soluble components of PM<sub>2.5</sub>  
408 was higher in the north than in the south. The correlation between DTT<sub>v</sub> and soluble  
409 elements was higher than that between DTT<sub>v</sub> and total elements in both the south and  
410 north. In the north, the DTT<sub>v</sub> was strongly correlated with soluble Mn, Co, Ni, Zn, As,  
411 Cd and Pb ( $r > 0.7$ ), and in the south it positively correlated with Mn, Fe, Cr, Co, As  
412 and Pb ( $r > 0.5$ ). In addition, in the north the DTT<sub>v</sub> was also positively correlated with  
413 WSOC, Abs<sub>365</sub> and NACs ( $r$  of 0.56 to 0.79), while in the south it was weakly  
414 correlated ( $r \leq 0.4$ ). These results indicate that in the north trace elements and water-  
415 soluble organic compounds, especially BrC chromophores, both had significant  
416 contributions to DTT consumption, and in the south the consumption of DTT may be  
417 mainly from trace elements. Six sources of DTT<sub>v</sub> were resolved with the PMF model,  
418 including biomass burning, coal burning, traffic-related, dust, oil combustion, and  
419 secondary formation. On average, traffic-related emissions (39.4%) and biomass  
420 burning (25.2%) were the major contributors of DTT<sub>v</sub> in the south, and traffic-related  
421 emissions (51.652%) was the predominated source in the north. The differences in  
422 DTT<sub>v</sub> sources in the south and north of Beijing suggest that the relationship between  
423 source emissions and atmospheric processes and PM<sub>2.5</sub> OP deserve further exploration  
424 in order to better understand the regional differences of health impacts of PM<sub>2.5</sub>.

425

426

427

428 **Date availability.** Raw data used in this study can be obtained from the following  
429 open link: <https://doi.org/10.5281/zenodo.10791126> (Yuan et al., 2024). It is also  
430 available on request by contacting the corresponding author.

431

432 **Supplement.** The Supplement related to this article is available online.

433

434 **Author contributions.** RJH designed the study. Data analysis was done by WY, CL,

435 LY, HY and RJH. WY, CL, LY, HY and RJH interpreted data, prepared the display  
436 items and wrote the manuscript. All authors commented on and discussed the  
437 manuscript.

438

439 **Competing interests.** The authors declare that they have no conflict of interest.

440

441 **Acknowledgements.** We are very grateful to the National Natural Science Foundation  
442 of China (NSFC) under Grant No. 41925015, the Strategic Priority Research Program  
443 of Chinese Academy of Sciences (XDB40000000), the Key Research Program of  
444 Frontier Sciences from the Chinese Academy of Sciences (ZDBS-LY-DQC001), the  
445 New Cornerstone Science Foundation through the XPLOER PRIZE, and the  
446 Postdoctoral Fellowship Program of CPSF (no. GZC20232628) supported this study.

447

448 **Financial support.** This work was supported by the National Natural Science  
449 Foundation of China (NSFC) under Grant No. 41925015, the Strategic Priority  
450 Research Program of Chinese Academy of Sciences (XDB40000000), the Key  
451 Research Program of Frontier Sciences from the Chinese Academy of Sciences  
452 (ZDBS-LY-DQC001), the New Cornerstone Science Foundation through the  
453 XPLOER PRIZE, and the Postdoctoral Fellowship Program of CPSF (no.  
454 GZC20232628).

455

456

## 457 **References**

458 Ahmad, M., Yu, Q., Chen, J., Cheng, S., Qin, W., and Zhang, Y.: Chemical  
459 characteristics, oxidative potential, and sources of PM<sub>2.5</sub> in wintertime in  
460 Lahore and Peshawar, Pakistan, *J. Environ. Sci.*, 102, 148-158,  
461 10.1016/j.jes.2020.09.014, 2021.

462 Al-Naiema, I. M. and Stone, E. A.: Evaluation of anthropogenic secondary organic  
463 aerosol tracers from aromatic hydrocarbons, *Atmos. Chem. Phys.*, 17, 2053-



464 2065, 10.5194/acp-17-2053-2017, 2017.

465 An, Z., Huang, R. J., Zhang, R., Tie, X., Li, G., Cao, J., Zhou, W., Shi, Z., Han, Y., Gu,  
466 Z., and Ji, Y.: Severe haze in northern China: A synergy of anthropogenic  
467 emissions and atmospheric processes, *Proc. Natl. Acad. Sci. U. S. A.*, 116,  
468 8657-8666, 10.1073/pnas.1900125116, 2019.

469 Bates, J. T., Fang, T., Verma, V., Zeng, L., Weber, R. J., Tolbert, P. E., Abrams, J. Y.,  
470 Sarnat, S. E., Klein, M., Mulholland, J. A., and Russell, A. G.: Review of  
471 Acellular Assays of Ambient Particulate Matter Oxidative Potential: Methods  
472 and Relationships with Composition, Sources, and Health Effects, *Environ.*  
473 *Sci. Technol.*, 53, 4003-4019, 10.1021/acs.est.8b03430, 2019.

474 ~~Belis, C., Larsen, B. R., Amato, F., Haddad, I. El, Favez, O., Harrison, R. M., Hopke,~~  
475 ~~P. K., Nava, S., Paatero, P., Prévôt, A., Quass, U., Vecchi, R., and Viana, M.:~~  
476 ~~European Guide on Air Pollution Source Apportionment with Receptor~~  
477 ~~Models, JRC References Report, March, 88, 1-170,~~  
478 ~~<https://doi.org/10.2788/9307>, 2019.~~

479 Burnett, R., Chen, H., Szyszkowicz, M., Fann, N., Hubbell, B., Pope, C. A., 3rd, Apte,  
480 J. S., Brauer, M., Cohen, A., Weichenthal, S., Coggins, J., Di, Q., Brunekreef,  
481 B., Frostad, J., Lim, S. S., Kan, H., Walker, K. D., Thurston, G. D., Hayes, R.  
482 B., Lim, C. C., Turner, M. C., Jerrett, M., Krewski, D., Gapstur, S. M., Diver,  
483 W. R., Ostro, B., Goldberg, D., Crouse, D. L., Martin, R. V., Peters, P., Pinault,  
484 L., Tjepkema, M., van Donkelaar, A., Villeneuve, P. J., Miller, A. B., Yin, P.,  
485 Zhou, M., Wang, L., Janssen, N. A. H., Marra, M., Atkinson, R. W., Tsang, H.,  
486 Quoc Thach, T., Cannon, J. B., Allen, R. T., Hart, J. E., Laden, F., Cesaroni, G.,  
487 Forastiere, F., Weinmayr, G., Jaensch, A., Nagel, G., Concin, H., and Spadaro,  
488 J. V.: Global estimates of mortality associated with long-term exposure to  
489 outdoor fine particulate matter, *Proc. Natl. Acad. Sci. U. S. A.*, 115, 9592-9597,  
490 10.1073/pnas.1803222115, 2018.

491 Calas, A., Uzu, G., Kelly, F. J., Houdier, S., Martins, J. M. F., Thomas, F., Molton, F.,  
492 Charron, A., Dunster, C., Oliete, A., Jacob, V., Besombes, J.-L., Chevrier, F.,

493 and Jaffrezo, J.-L.: Comparison between five acellular oxidative potential  
494 measurement assays performed with detailed chemistry on PM<sub>10</sub> samples from  
495 the city of Chamonix (France), *Atmos. Chem. Phys.*, 18, 7863-7875,  
496 10.5194/acp-18-7863-2018, 2018.

497 Campbell, S. J., Wolfer, K., Utinger, B., Westwood, J., Zhang, Z. H., Bukowiecki, N.,  
498 Steimer, S. S., Vu, T. V., Xu, J., Straw, N., Thomson, S., Elzein, A., Sun, Y.,  
499 Liu, D., Li, L., Fu, P., Lewis, A. C., Harrison, R. M., Bloss, W. J., Loh, M.,  
500 Miller, M. R., Shi, Z., and Kalberer, M.: Atmospheric conditions and  
501 composition that influence PM<sub>2.5</sub> oxidative potential in Beijing, China, *Atmos.*  
502 *Chem. Phys.*, 21, 5549-5573, 10.5194/acp-21-5549-2021, 2021.

503 Cao, T., Li, M., Zou, C., Fan, X., Song, J., Jia, W., Yu, C., Yu, Z., and Peng, P. a.:  
504 Chemical composition, optical properties, and oxidative potential of water-  
505 and methanol-soluble organic compounds emitted from the combustion of  
506 biomass materials and coal, *Atmos. Chem. Phys.*, 21, 13187-13205,  
507 10.5194/acp-21-13187-2021, 2021.

508 Charrier, J. G. and Anastasio, C.: On dithiothreitol (DTT) as a measure of oxidative  
509 potential for ambient particles: evidence for the importance of soluble  
510 transition metals, *Atmos. Chem. Phys.*, 12, 9321-9333, 10.5194/acp-12-9321-  
511 2012, 2012.

512 Charrier, J. G., McFall, A. S., Vu, K. K.-T., Baroi, J., Olea, C., Hasson, A., and  
513 Anastasio, C.: A Bias in the “Mass-Normalized” DTT Response-An Effect of  
514 Non-Linear Concentration Response Curves for Copper and Manganese,  
515 *Atmos. Environ.*, 144, 325-334, 2016.

516 Chen, K., Xu, J., Famiyeh, L., Sun, Y., Ji, D., Xu, H., Wang, C., Metcalfe, S. E., Betha,  
517 R., Behera, S. N., Jia, C., Xiao, H., and He, J.: Chemical constituents, driving  
518 factors, and source apportionment of oxidative potential of ambient fine  
519 particulate matter in a Port City in East China, *J. Hazard. Mater.*, 440,  
520 10.1016/j.jhazmat.2022.129864, 2022.

521 Chen, Q., Wang, M., Wang, Y., Zhang, L., Li, Y., and Han, Y.: Oxidative Potential of

522 Water-Soluble Matter Associated with Chromophoric Substances in PM<sub>2.5</sub>  
523 over Xi'an, China, *Environ. Sci. Technol.*, 53, 8574-8584,  
524 10.1021/acs.est.9b01976, 2019.

525 Chirizzi, D., Cesari, D., Guascito, M. R., Dinoi, A., Giotta, L., Donateo, A., and  
526 Contini, D.: Influence of Saharan dust outbreaks and carbon content on  
527 oxidative potential of water-soluble fractions of PM<sub>2.5</sub> and PM<sub>10</sub>, *Atmos.*  
528 *Environ.*, 163, 1-8, 10.1016/j.atmosenv.2017.05.021, 2017.

529 Chow, W. S., Huang, X. H. H., Leung, K. F., Huang, L., Wu, X., and Yu, J. Z.:  
530 Molecular and elemental marker-based source apportionment of fine  
531 particulate matter at six sites in Hong Kong, China, *Sci. Total Environ.*, 813,  
532 152652, 10.1016/j.scitotenv.2021.152652, 2022.

533 Chowdhury, P. H., He, Q., Carmieli, R., Li, C., Rudich, Y., and Pardo, M.: Connecting  
534 the Oxidative Potential of Secondary Organic Aerosols with Reactive Oxygen  
535 Species in Exposed Lung Cells, *Environ. Sci. Technol.*, 53, 13949-13958,  
536 10.1021/acs.est.9b04449, 2019.

537 Cui, Y., Zhu, L., Wang, H., Zhao, Z., Ma, S., and Ye, Z.: Characteristics and Oxidative  
538 Potential of Ambient PM<sub>2.5</sub> in the Yangtze River Delta Region: Pollution Level  
539 and Source Apportionment, *Atmosphere*, 14, 10.3390/atmos14030425, 2023.

540 Daellenbach, K. R., Uzu, G., Jiang, J., Cassagnes, L. E., Leni, Z., Vlachou, A.,  
541 Stefanelli, G., Canonaco, F., Weber, S., Segers, A., Kuenen, J. J. P., Schaap, M.,  
542 Favez, O., Albinet, A., Aksoyoglu, S., Dommen, J., Baltensperger, U., Geiser,  
543 M., El Haddad, I., Jaffrezo, J. L., and Prevot, A. S. H.: Sources of particulate-  
544 matter air pollution and its oxidative potential in Europe, *Nature*, 587, 414-419,  
545 10.1038/s41586-020-2902-8, 2020.

546 Fan, X., Li, M., Cao, T., Cheng, C., Li, F., Xie, Y., Wei, S., Song, J., and Peng, P. a.:  
547 Optical properties and oxidative potential of water- and alkaline-soluble  
548 brown carbon in smoke particles emitted from laboratory simulated biomass  
549 burning, *Atmos. Environ.*, 194, 48-57, 10.1016/j.atmosenv.2018.09.025, 2018.

550 Fang, T., Verma, V., Bates, J. T., Abrams, J., Klein, M., Strickland, M. J., Sarnat, S. E.,

551 Chang, H. H., Mulholland, J. A., Tolbert, P. E., Russell, A. G., and Weber, R. J.:  
552 Oxidative potential of ambient water-soluble PM<sub>2.5</sub> in the southeastern United  
553 States: contrasts in sources and health associations between ascorbic acid (AA)  
554 and dithiothreitol (DTT) assays, *Atmos. Chem. Phys.*, 16, 3865-3879,  
555 10.5194/acp-16-3865-2016, 2016.

556 Feng, R., Xu, H., Gu, Y., Wang, Z., Han, B., Sun, J., Liu, S., Lu, H., Ho, S. S. H.,  
557 Shen, Z., and Cao, J.: Variations of Personal Exposure to Particulate Nitrated  
558 Phenols from Heating Energy Renovation in China: The First Assessment on  
559 Associated Toxicological Impacts with Particle Size Distributions, *Environ.*  
560 *Sci. Technol.*, 56, 3974–3983, 2022.

561 Gao, D., Fang, T., Verma, V., Zeng, L., and Weber, R. J.: A method for measuring total  
562 aerosol oxidative potential (OP) with the dithiothreitol (DTT) assay and  
563 comparisons between an urban and roadside site of water-soluble and total OP,  
564 *Atmos. Meas. Tech.*, 10, 2821-2835, 10.5194/amt-10-2821-2017, 2017.

565 Hecobian, A., Zhang, X., Zheng, M., Frank, N., Edgerton, E. S., and Weber, R. J.:  
566 Water-Soluble Organic Aerosol material and the light-absorption  
567 characteristics of aqueous extracts measured over the Southeastern United  
568 States, *Atmos. Chem. Phys.*, 10, 5965-5977, 10.5194/acp-10-5965-2010, 2010.

569 Ho, K. F., Ho, S. S. H., Huang, R.-J., Liu, S. X., Cao, J.-J., Zhang, T., Chuang, H.-C.,  
570 Chan, C. S., Hu, D., and Tian, L.: Characteristics of water-soluble organic  
571 nitrogen in fine particulate matter in the continental area of China, *Atmos.*  
572 *Environ.*, 106, 252-261, 10.1016/j.atmosenv.2015.02.010, 2015.

573 Huang, R. J., Cheng, R., Jing, M., Yang, L., Li, Y., Chen, Q., Chen, Y., Yan, J., Lin, C.,  
574 Wu, Y., Zhang, R., El Haddad, I., Prevot, A. S. H., O'Dowd, C. D., and Cao, J.:  
575 Source-Specific Health Risk Analysis on Particulate Trace Elements: Coal  
576 Combustion and Traffic Emission As Major Contributors in Wintertime  
577 Beijing, *Environ. Sci. Technol.*, 52, 10967-10974, 10.1021/acs.est.8b02091,  
578 2018.

579 Huang, R. J., Yang, L., Shen, J., Yuan, W., Gong, Y., Guo, J., Cao, W., Duan, J., Ni, H.,

580 Zhu, C., Dai, W., Li, Y., Chen, Y., Chen, Q., Wu, Y., Zhang, R., Dusek, U.,  
581 O'Dowd, C., and Hoffmann, T.: Water-Insoluble Organics Dominate Brown  
582 Carbon in Wintertime Urban Aerosol of China: Chemical Characteristics and  
583 Optical Properties, *Environ. Sci. Technol.*, 54, 7836-7847,  
584 10.1021/acs.est.0c01149, 2020.

585 Huang, R. J., Zhang, Y., Bozzetti, C., Ho, K. F., Cao, J. J., Han, Y., Daellenbach, K. R.,  
586 Slowik, J. G., Platt, S. M., Canonaco, F., Zotter, P., Wolf, R., Pieber, S. M.,  
587 Bruns, E. A., Crippa, M., Ciarelli, G., Piazzalunga, A., Schwikowski, M.,  
588 Abbaszade, G., Schnelle-Kreis, J., Zimmermann, R., An, Z., Szidat, S.,  
589 Baltensperger, U., El Haddad, I., and Prevot, A. S.: High secondary aerosol  
590 contribution to particulate pollution during haze events in China, *Nature*, 514,  
591 218-222, 10.1038/nature13774, 2014.

592 Jiang, H., Xie, Y., Ge, Y., He, H., and Liu, Y.: Effects of ultrasonic treatment on  
593 dithiothreitol (DTT) assay measurements for carbon materials, *J. Environ. Sci.*,  
594 84, 51–58, 2019.

595 Joo, H. S., Batmunkh, T., Borlaza, L. J. S., Park, M., Lee, K. Y., Lee, J. Y., Chang, Y.  
596 W., and Park, K.: Physicochemical properties and oxidative potential of fine  
597 particles produced from coal combustion, *Aerosol Sci. Technol.*, 52, 1134-  
598 1144, 10.1080/02786826.2018.1501152, 2018.

599 Khoshnamvand, N., Nodehi, R. N., Hassanvand, M. S., and Naddafi, K.: Comparison  
600 between oxidative potentials measured of water-soluble components in  
601 ambient air PM<sub>1</sub> and PM<sub>2.5</sub> of Tehran, Iran, *Air Qual. Atmos. Hlth.*, 16, 1311-  
602 1320, 10.1007/s11869-023-01343-y, 2023.

603 Laskin, A., Laskin, J., and Nizkorodov, S. A.: Chemistry of atmospheric brown carbon,  
604 *Chem. Rev.*, 115, 4335-4382, 10.1021/cr5006167, 2015.

605 Lelieveld, S., Wilson, J., Dovrou, E., Mishra, A., Lakey, P. S. J., Shiraiwa, M., Poschl,  
606 U., and Berkemeier, T.: Hydroxyl Radical Production by Air Pollutants in  
607 Epithelial Lining Fluid Governed by Interconversion and Scavenging of  
608 Reactive Oxygen Species, *Environ. Sci. Technol.*, 55, 14069-14079,

609 10.1021/acs.est.1c03875, 2021.

610 Lin, P., Bluvshstein, N., Rudich, Y., Nizkorodov, S. A., Laskin, J., and Laskin, A.:  
611 Molecular chemistry of atmospheric brown carbon inferred from a nationwide  
612 biomass burning event, *Environ. Sci. Technol.*, 51, 11561–11570, 2017.

613 Liu, W., Xu, Y., Liu, W., Liu, Q., Yu, S., Liu, Y., Wang, X., and Tao, S.: Oxidative  
614 potential of ambient PM<sub>2.5</sub> in the coastal cities of the Bohai Sea, northern  
615 China: Seasonal variation and source apportionment, *Environ. Pollut.*, 236,  
616 514-528, 10.1016/j.envpol.2018.01.116, 2018.

617 Liu, Y., Yan, C. Q., Ding, X., Wang, X. M., Fu, Q. Y., Zhao, Q. B., Zhang, Y. H., Duan,  
618 Y. S., Qiu, X. H., and Zheng, M.: Sources and spatial distribution of  
619 particulate polycyclic aromatic hydrocarbons in Shanghai, China, *Sci. Total  
620 Environ.*, 584-585, 307-317, <https://doi.org/10.1016/j.scitotenv.2016.12.134>,  
621 2017.

622 Ma, X., Nie, D., Chen, M., Ge, P., Liu, Z., Ge, X., Li, Z., and Gu, R.: The Relative  
623 Contributions of Different Chemical Components to the Oxidative Potential of  
624 Ambient Fine Particles in Nanjing Area, *Int. J. Environ. Res. Public Health*, 18,  
625 2789, 10.3390/ijerph18062789, 2021.

626 Miljevic, B., Hedayat, F., Stevanovic, S., Fairfull-Smith, K. E., Bottle, S. E., and  
627 Ristovski, Z. D.: To sonicate or not to sonicate PM filters: reactive oxygen  
628 species generation upon ultrasonic irradiation, *Aerosol. Sci. Technol.*, 48,  
629 1276-1284, 2014.

630 Minguillón, M. C., Cirach, M., Hoek, G., Brunekreef, B., Tsai, M., de Hoogh, K.,  
631 Jedynska, A., Kooter, I. M., Nieuwenhuijsen, M., and Querol, X.: Spatial  
632 variability of trace elements and sources for improved exposure assessment in  
633 Barcelona, *Atmos. Environ.*, 89, 268-281, 10.1016/j.atmosenv.2014.02.047,  
634 2014.

635 Moreno, T., Querol, X., Alastuey, A., Reche, C., Cusack, M., Amato, F., Pandolfi, M.,  
636 Pey, J., Richard, A., Prévôt, A. S. H., Furger, M., and Gibbons, W.: Variations  
637 in time and space of trace metal aerosol concentrations in urban areas and their

638 surroundings, *Atmos. Chem. Phys.*, 11, 9415-9430, 10.5194/acp-11-9415-2011,  
639 2011.

640 Oh, S. H., Park, K., Park, M., Song, M., Jang, K. S., Schauer, J. J., Bae, G. N., and  
641 Bae, M. S.: Comparison of the sources and oxidative potential of PM<sub>2.5</sub> during  
642 winter time in large cities in China and South Korea, *Sci. Total Environ.*, 859,  
643 160369, 10.1016/j.scitotenv.2022.160369, 2023.

644 Paatero, P.: Least squares formation of robust non negative factor analysis,  
645 *Chemometr. Intell. Lab.*, 37, 23-35, 1997.

646 Puthussery, J. V., Dave, J., Shukla, A., Gaddamidi, S., Singh, A., Vats, P., Salana, S.,  
647 Ganguly, D., Rastogi, N., Tripathi, S. N., and Verma, V.: Effect of Biomass  
648 Burning, Diwali Fireworks, and Polluted Fog Events on the Oxidative  
649 Potential of Fine Ambient Particulate Matter in Delhi, India, *Environ. Sci.*  
650 *Technol.*, 56, 14605-14616, 10.1021/acs.est.2c02730, 2022.

651 Shen, J., Taghvaei, S., La, C., Oroumijeh, F., Liu, J., Jerrett, M., Weichenthal, S., Del  
652 Rosario, I., Shafer, M. M., Ritz, B., Zhu, Y., and Paulson, S. E.: Aerosol  
653 Oxidative Potential in the Greater Los Angeles Area: Source Apportionment  
654 and Associations with Socioeconomic Position, *Environ. Sci. Technol.*, 56,  
655 17795-17804, 10.1021/acs.est.2c02788, 2022.

656 Ting, Y. C., Chang, P. K., Hung, P. C., Chou, C. C., Chi, K. H., and Hsiao, T. C.:  
657 Characterizing emission factors and oxidative potential of motorcycle  
658 emissions in a real-world tunnel environment, *Environ. Res.*, 234, 116601,  
659 10.1016/j.envres.2023.116601, 2023.

660 Tong, H., Lakey, P. S. J., Arangio, A. M., Socorro, J., Kampf, C. J., Berkemeier, T.,  
661 Brune, W. H., Poschl, U., and Shiraiwa, M.: Reactive oxygen species formed  
662 in aqueous mixtures of secondary organic aerosols and mineral dust  
663 influencing cloud chemistry and public health in the Anthropocene, *Faraday*  
664 *Discuss.*, 200, 251-270, 10.1039/c7fd00023e, 2017.

665 Tong, H., Lakey, P. S. J., Arangio, A. M., Socorro, J., Shen, F., Lucas, K., Brune, W.  
666 H., Poschl, U., and Shiraiwa, M.: Reactive Oxygen Species Formed by

667 Secondary Organic Aerosols in Water and Surrogate Lung Fluid, *Environ. Sci.*  
668 *Technol.*, 52, 11642-11651, 10.1021/acs.est.8b03695, 2018.

669 Tuet, W. Y., Chen, Y., Xu, L., Fok, S., Gao, D., Weber, R. J., and Ng, N. L.: Chemical  
670 oxidative potential of secondary organic aerosol (SOA) generated from the  
671 photooxidation of biogenic and anthropogenic volatile organic compounds,  
672 *Atmos. Chem. Phys.*, 17, 839-853, 10.5194/acp-17-839-2017, 2017.

673 Tuet, W. Y., Liu, F., de Oliveira Alves, N., Fok, S., Artaxo, P., Vasconcellos, P.,  
674 Champion, J. A., and Ng, N. L.: Chemical Oxidative Potential and Cellular  
675 Oxidative Stress from Open Biomass Burning Aerosol, *Environ. Sci. Technol.*  
676 *Lett.*, 6, 126-132, 10.1021/acs.estlett.9b00060, 2019.

677 Verma, V., Fang, T., Xu, L., Peltier, R. E., Russell, A. G., Ng, N. L., and Weber, R. J.:  
678 Organic aerosols associated with the generation of reactive oxygen species  
679 (ROS) by water-soluble PM<sub>2.5</sub>, *Environ. Sci. Technol.*, 49, 4646-4656,  
680 10.1021/es505577w, 2015.

681 Verma, V., Rico-Martinez, R., Kotra, N., King, L., Liu, J., Snell, T. W., and Weber, R.  
682 J.: Contribution of water-soluble and insoluble components and their  
683 hydrophobic/hydrophilic subfractions to the reactive oxygen species-  
684 generating potential of fine ambient aerosols, *Environ. Sci. Technol.*, 46,  
685 11384-11392, 10.1021/es302484r, 2012.

686 Verma, V., Fang, T., Guo, H., King, L., Bates, J. T., Peltier, R. E., Edgerton, E.,  
687 Russell, A. G., and Weber, R. J.: Reactive oxygen species associated with  
688 water-soluble PM<sub>2.5</sub> in the southeastern United States: spatiotemporal trends  
689 and source apportionment, *Atmos. Chem. Phys.*, 14, 12915-12930,  
690 10.5194/acp-14-12915-2014, 2014.

691 Vreeland, H., Weber, R., Bergin, M., Greenwald, R., Golan, R., Russell, A. G., Verma,  
692 V., and Sarnat, J. A.: Oxidative potential of PM<sub>2.5</sub> during Atlanta rush hour:  
693 Measurements of in-vehicle dithiothreitol (DTT) activity, *Atmos. Environ.*,  
694 165, 169-178, 10.1016/j.atmosenv.2017.06.044, 2017.

695 Wang, J., Lin, X., Lu, L., Wu, Y., Zhang, H., Lv, Q., Liu, W., Zhang, Y., and Zhuang,



696 S.: Temporal variation of oxidative potential of water soluble components of  
697 ambient PM<sub>2.5</sub> measured by dithiothreitol (DTT) assay, *Sci. Total Environ.*,  
698 649, 969-978, 10.1016/j.scitotenv.2018.08.375, 2019.

699 Wang, T., Huang, R. J., Li, Y., Chen, Q., Chen, Y., Yang, L., Guo, J., Ni, H., Hoffmann,  
700 T., Wang, X., and Mai, B.: One-year characterization of organic aerosol  
701 markers in urban Beijing: Seasonal variation and spatiotemporal comparison,  
702 *Sci. Total Environ.*, 743, 140689, 10.1016/j.scitotenv.2020.140689, 2020a.

703 Wang, Y., Wang, M., Li, S., Sun, H., Mu, Z., Zhang, L., Li, Y., and Chen, Q.: Study on  
704 the oxidation potential of the water-soluble components of ambient PM<sub>2.5</sub> over  
705 Xi'an, China: Pollution levels, source apportionment and transport pathways,  
706 *Environ. Int.*, 136, 105515, 10.1016/j.envint.2020.105515, 2020b.

707 Wong, J. P. S., Tsagkaraki, M., Tsiodra, I., Mihalopoulos, N., Violaki, K., Kanakidou,  
708 M., Sciare, J., Nenes, A., and Weber, R. J.: Effects of Atmospheric Processing  
709 on the Oxidative Potential of Biomass Burning Organic Aerosols, *Environ. Sci.*  
710 *Technol.*, 53, 6747-6756, 10.1021/acs.est.9b01034, 2019.

711 Wu, N., Lu, B., Chen, Q., Chen, J., and Li, X.: Connecting the Oxidative Potential of  
712 Fractionated Particulate Matter With Chromophoric Substances, *J. Geophys.*  
713 *Res-Atmos.*, 127, 10.1029/2021jd035503, 2022a.

714 Wu, N., Lyu, Y., Lu, B., Cai, D., Meng, X., and Li, X.: Oxidative potential induced by  
715 metal-organic interaction from PM<sub>2.5</sub> in simulated biological fluids, *Sci. Total*  
716 *Environ.*, 848, 157768, 10.1016/j.scitotenv.2022.157768, 2022b.

717 Xing, C., Wang, Y., Yang, X., Zeng, Y., Zhai, J., Cai, B., Zhang, A., Fu, T. M., Zhu, L.,  
718 Li, Y., Wang, X., and Zhang, Y.: Seasonal variation of driving factors of  
719 ambient PM<sub>2.5</sub> oxidative potential in Shenzhen, China, *Sci. Total Environ.*, 862,  
720 160771, 10.1016/j.scitotenv.2022.160771, 2023.

721 Xiong, Q., Yu, H., Wang, R., Wei, J., and Verma, V.: Rethinking Dithiothreitol-Based  
722 Particulate Matter Oxidative Potential: Measuring Dithiothreitol Consumption  
723 versus Reactive Oxygen Species Generation, *Environ. Sci. Technol.*, 51, 6507-  
724 6514, 10.1021/acs.est.7b01272, 2017.

725 Yalamanchili, J., Hennigan, C. J., and Reed, B. E.: Measurement artifacts in the  
726 dithiothreitol (DTT) oxidative potential assay caused by interactions between  
727 aqueous metals and phosphate buffer, *J. Hazard. Mater.*, 456, 131693, 2023.

728 Yu, H., Wei, J., Cheng, Y., Subedi, K., and Verma, V.: Synergistic and Antagonistic  
729 Interactions among the Particulate Matter Components in Generating Reactive  
730 Oxygen Species Based on the Dithiothreitol Assay, *Environ. Sci. Technol.*, 52,  
731 2261–2270, 2018.

732 Yu, Q., Chen, J., Qin, W., Ahmad, M., Zhang, Y., Sun, Y., Xin, K., and Ai, J.:  
733 Oxidative potential associated with water-soluble components of PM<sub>2.5</sub> in  
734 Beijing: The important role of anthropogenic organic aerosols, *J. Hazard.  
735 Mater.*, 433, 128839, 10.1016/j.jhazmat.2022.128839, 2022a.

736 Yu, S., Liu, W., Xu, Y., Yi, K., Zhou, M., Tao, S., and Liu, W.: Characteristics and  
737 oxidative potential of atmospheric PM<sub>2.5</sub> in Beijing: Source apportionment and  
738 seasonal variation, *Sci. Total Environ.*, 650, 277-287,  
739 10.1016/j.scitotenv.2018.09.021, 2019.

740 Yu, Y., Sun, Q., Li, T., Ren, X., Lin, L., Sun, M., Duan, J., and Sun, Z.: Adverse  
741 outcome pathway of fine particulate matter leading to increased cardiovascular  
742 morbidity and mortality: An integrated perspective from toxicology and  
743 epidemiology, *J. Hazard. Mater.*, 430, 128368, 10.1016/j.jhazmat.2022.128368,  
744 2022b.

745 Yu, Y., Cheng, P., Li, Y., Gu, J., Gong, Y., Han, B., Yang, W., Sun, J., Wu, C., Song,  
746 W., and Li, M.: The association of chemical composition particularly the  
747 heavy metals with the oxidative potential of ambient PM<sub>2.5</sub> in a megacity  
748 (Guangzhou) of southern China, *Environ. Res.*, 213, 113489,  
749 10.1016/j.envres.2022.113489, 2022c.

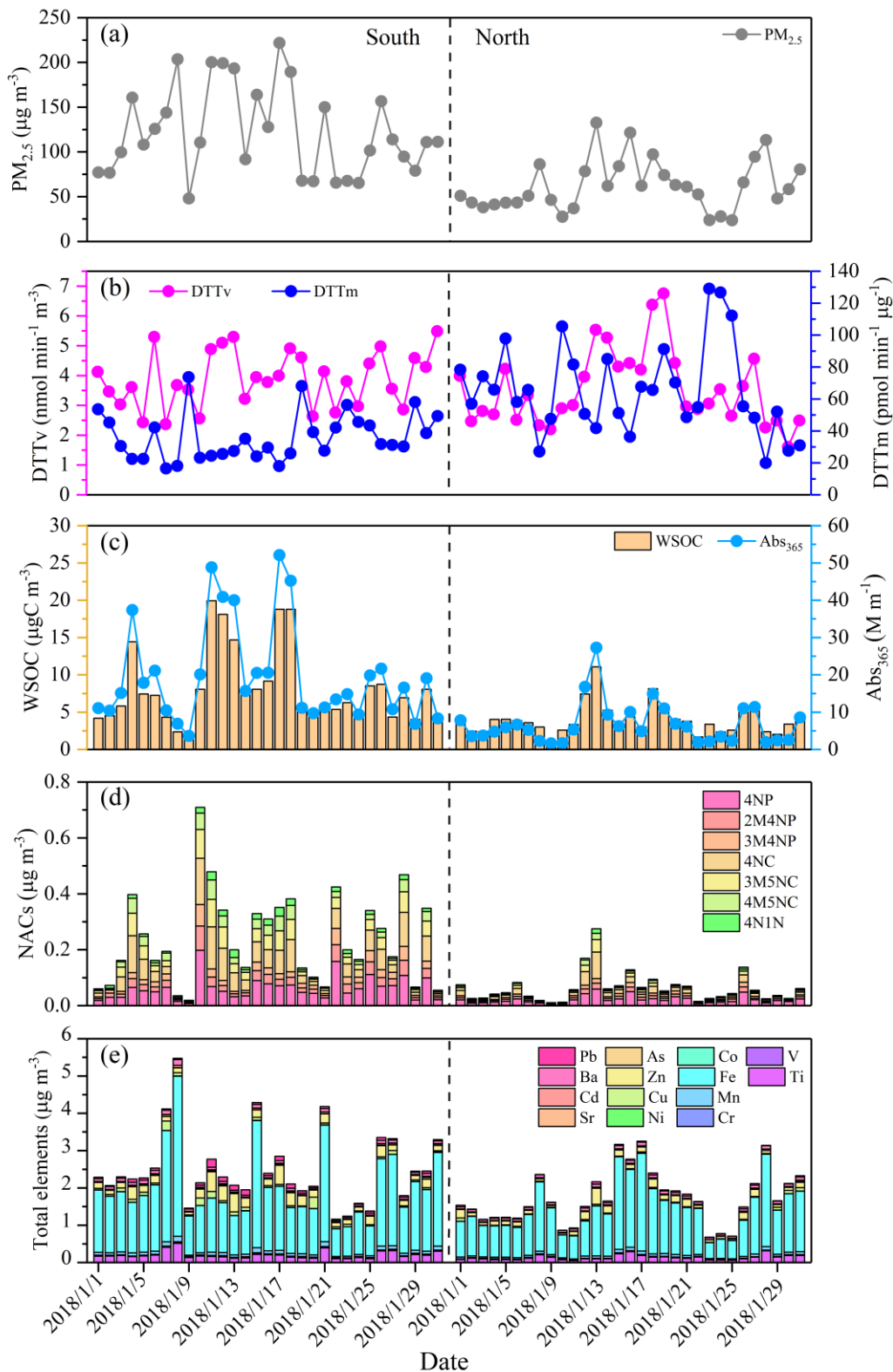
750 Yuan, W., Huang, R.-J., Luo, C., Yang, L., Cao, W., Guo, J., and Yang, H.:  
751 Measurement report: Oxidation potential of water-soluble aerosol components  
752 in the southern and northern of Beijing, Zenodo [data set],  
753 <https://doi.org/10.5281/zenodo.10791126>, 2024.

754 Yuan, W., Huang, R.-J., Yang, L., Guo, J., Chen, Z., Duan, J., Wang, T., Ni, H., Han,  
755 Y., Li, Y., Chen, Q., Chen, Y., Hoffmann, T., and O'Dowd, C.: Characterization  
756 of the light-absorbing properties, chromophore composition and sources of  
757 brown carbon aerosol in Xi'an, northwestern China, *Atmos. Chem. Phys.*, 20,  
758 5129-5144, 10.5194/acp-20-5129-2020, 2020.

759 Zhang, Q., Ma, H., Li, J., Jiang, H., Chen, W., Wan, C., Jiang, B., Dong, G., Zeng, X.,  
760 Chen, D., Lu, S., You, J., Yu, Z., Wang, X., and Zhang, G.: Nitroaromatic  
761 Compounds from Secondary Nitrate Formation and Biomass Burning Are  
762 Major Proinflammatory Components in Organic Aerosols in Guangzhou: A  
763 Bioassay Combining High-Resolution Mass Spectrometry Analysis, *Environ.*  
764 *Sci. Technol.*, 57, 21570-21580, <https://doi.org/10.1021/acs.est.3c04983>, 2023.

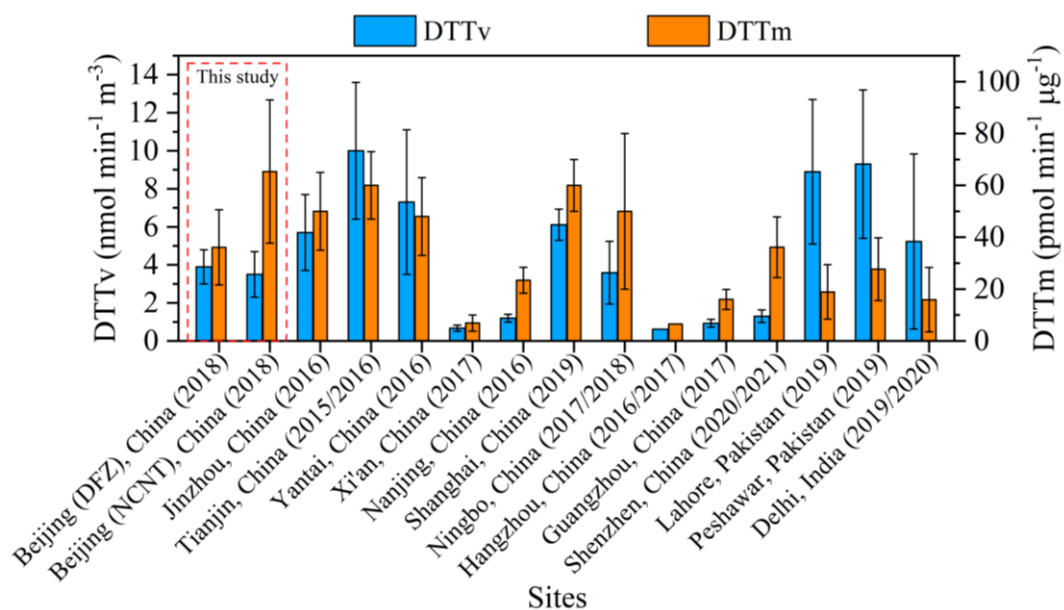
765 Zheng, Y., Davis, S. J., Persad, G. G., and Caldeira, K.: Climate effects of aerosols  
766 reduce economic inequality, *Nat. Clim. Chang.*, 10, 220-224, 2020.

767  
768  
769  
770



771

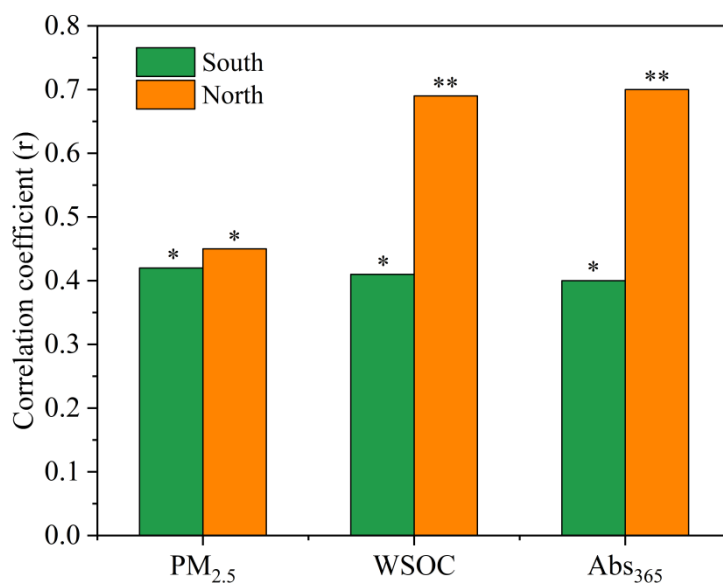
772 **Figure 1.** Time series of (a) PM<sub>2.5</sub> concentration, (b) DTT<sub>v</sub> and DTT<sub>m</sub>, (c)  
 773 concentration and light absorption at wavelength 365 nm (Abs<sub>365</sub>) of WSOC,  
 774 concentrations of (d) NACs and (e) elements.



775

776 **Figure 2.** Comparison of  $DTT_v$  and  $DTT_m$  values of water-soluble  $PM_{2.5}$  measured in  
 777 this study with those measured in other areas of Asia during similar period.

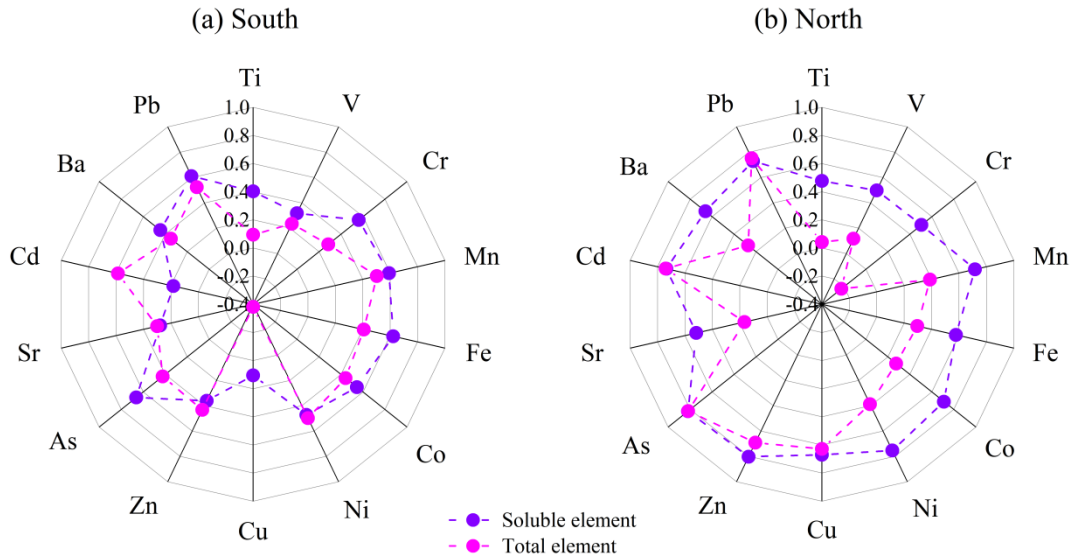
778



779

780 **Figure 3.** Correlation coefficients between  $DTT_v$  and  $PM_{2.5}$ , WSOC, and  $Abs_{365}$  in the  
 781 south and north of Beijing (\* indicates correlation is significant at the 0.05 level, and  
 782 \*\* indicates correlation is significant at the 0.01 level).

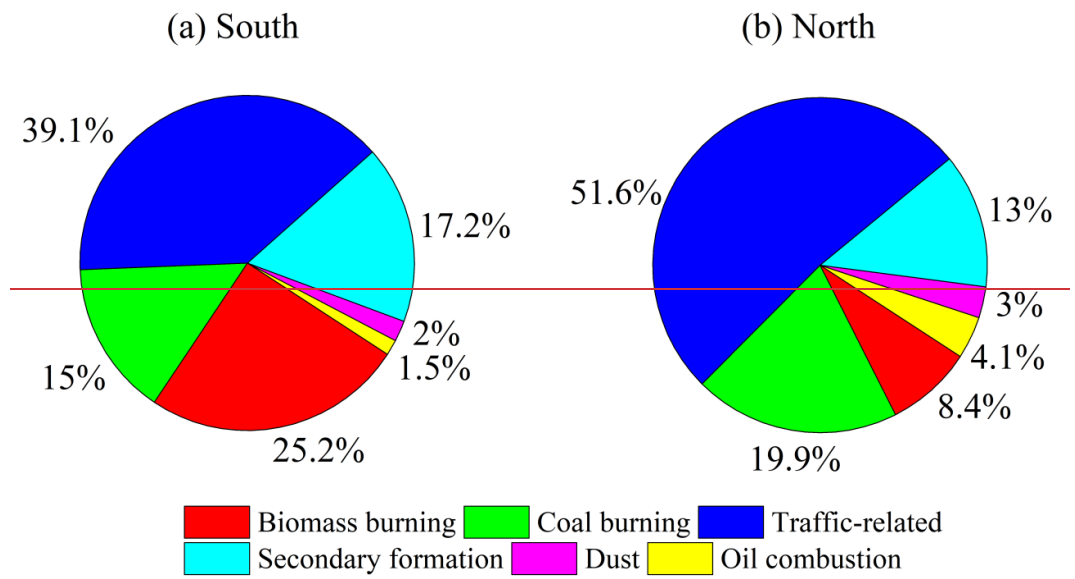
783



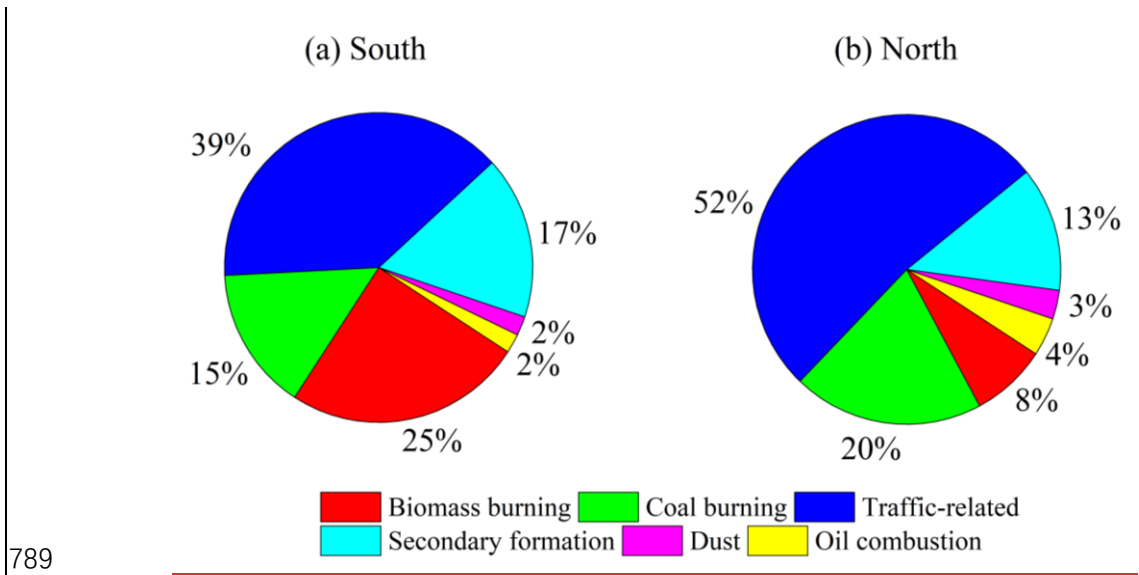
784

785 **Figure 4.** Correlation coefficients between  $DTT_v$  and elements in the (a) south and (b)  
 786 north of Beijing.

787



788



789

790 **Figure 5.** Contributions of resolved sources to DTT<sub>v</sub> in the (a) south and (b) north of  
 791 Beijing.